



Heriot-Watt University
Research Gateway

Mid-infrared laser emission from Fe

Citation for published version:

Lancaster, A, Cook, G, McDaniel, SA, Evans, J, Berry, PA, Shephard, JD & Kar, AK 2015, 'Mid-infrared laser emission from Fe: ZnSe cladding waveguides', *Applied Physics Letters*, vol. 107, no. 3, 031108. <https://doi.org/10.1063/1.4927384>

Digital Object Identifier (DOI):

[10.1063/1.4927384](https://doi.org/10.1063/1.4927384)

Link:

[Link to publication record in Heriot-Watt Research Portal](#)

Document Version:

Publisher's PDF, also known as Version of record

Published In:

Applied Physics Letters

Publisher Rights Statement:

© 2015 Author(s). All article content, except where otherwise noted, is licensed under a Creative Commons Attribution 3.0 Unported License.

General rights

Copyright for the publications made accessible via Heriot-Watt Research Portal is retained by the author(s) and / or other copyright owners and it is a condition of accessing these publications that users recognise and abide by the legal requirements associated with these rights.

Take down policy

Heriot-Watt University has made every reasonable effort to ensure that the content in Heriot-Watt Research Portal complies with UK legislation. If you believe that the public display of this file breaches copyright please contact open.access@hw.ac.uk providing details, and we will remove access to the work immediately and investigate your claim.

Mid-infrared laser emission from Fe:ZnSe cladding waveguides

A. Lancaster, G. Cook, S. A. McDaniel, J. Evans, P. A. Berry, J. D. Shephard, and A. K. Kar

Citation: [Applied Physics Letters](#) **107**, 031108 (2015); doi: 10.1063/1.4927384

View online: <http://dx.doi.org/10.1063/1.4927384>

View Table of Contents: <http://scitation.aip.org/content/aip/journal/apl/107/3?ver=pdfcov>

Published by the [AIP Publishing](#)

Articles you may be interested in

[Mid-infrared light emission from a Fe²⁺:ZnSe polycrystal using quantum cascade laser pumping](#)

Appl. Phys. Lett. **105**, 141108 (2014); 10.1063/1.4897546

[Compact mid-infrared Cr:ZnSe channel waveguide laser](#)

Appl. Phys. Lett. **102**, 161110 (2013); 10.1063/1.4803058

[A magnifying fiber element with an array of sub-wavelength Ge/ZnSe pixel waveguides for infrared imaging](#)

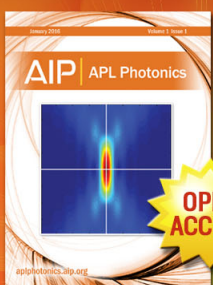
Appl. Phys. Lett. **101**, 021108 (2012); 10.1063/1.4734787

[Photopumped green lasing on BeZnSeTe double heterostructures grown on InP substrates](#)

Appl. Phys. Lett. **94**, 021104 (2009); 10.1063/1.3058761

[Yellow-green ZnCdSe/BeZnTe II-VI laser diodes grown on InP substrates](#)

Appl. Phys. Lett. **81**, 972 (2002); 10.1063/1.1492311



Launching in 2016!

The future of applied photonics research is here

AIP | APL
Photonics

Mid-infrared laser emission from Fe:ZnSe cladding waveguides

A. Lancaster,¹ G. Cook,² S. A. McDaniel,³ J. Evans,² P. A. Berry,² J. D. Shephard,¹
 and A. K. Kar^{1,a)}

¹*Institute of Photonics and Quantum Sciences, Heriot-Watt University, Edinburgh EH14 4AS, United Kingdom*

²*Air Force Research Laboratory, Sensors Directorate, Wright Patterson Air Force Base, Ohio 45433, USA*

³*Leidos, Inc., 3745 Pentagon Boulevard, Beavercreek, Ohio 45431, USA*

(Received 7 May 2015; accepted 12 July 2015; published online 22 July 2015)

The authors present a mid-IR depressed cladding waveguide laser in Fe:ZnSe. The laser produced a maximum output power of 76 mW at 4122 nm and laser thresholds as low as 154 mW were demonstrated. This represents a 44% reduction in threshold power compared with the bulk laser system demonstrated in this paper. The waveguide laser was found to have a narrow spectral linewidth of 6 nm FWHM compared to the 50 nm typical of bulk Fe:ZnSe lasers. © 2015 Author(s). All article content, except where otherwise noted, is licensed under a Creative Commons Attribution 3.0 Unported License. [<http://dx.doi.org/10.1063/1.4927384>]

Demand for widely tunable high-power mid-IR (2–5 μm) laser sources has driven the development of transition metal doped II–VI semiconductors laser sources since their first introduction into the photonics community by DeLoach *et al.*¹ The sources of this demand are many mid-IR sensing applications such as remote sensing, laser radar, and chemical detection. Ti-sapphire based systems can produce laser light over a very wide range in the mid-IR region when coupled with nonlinear crystals (OPOs), which add increased size, complexity, and cost to the system. Quantum Cascade Lasers (QCLs) offer direct light generation in the mid-IR but are limited to narrow tuning in the 2–5 μm ranges.^{2,3} For direct generation of laser light in the 2–3 μm region, the most developed gain medium is chromium-doped zinc selenide (Cr:ZnSe). Cr:ZnSe has demonstrated 30 W of output power and a continuous tunable range of 1973 nm–3249 nm.^{4,5} Iron-doped ZnSe (Fe:ZnSe) is another promising broad-band gain medium with luminescence from 3.5 to 5.2 μm at room temperature.⁶ The absorption and emission bands of Fe:ZnSe are shifted to longer wavelengths than that of Cr:ZnSe because the d^6 electron configuration of the Fe^{2+} ion experiences a 4/9 reduction in the magnitude of the crystal field splitting in ZnSe when compared to the d^4 configuration of the Cr^{2+} ion. The first Fe:ZnSe laser was demonstrated by Adams *et al.*⁷ Since then, CW output powers of >1.5 W, 35 W of average output power in gain switched operation, and tunable operation from 3770 to 5050 nm have been demonstrated in Fe:ZnSe lasers.^{4,8,9} One of the limitations of the Fe:ZnSe laser transition is the short upper-state lifetime at RT due to multiphonon quenching.⁷ The practical implication of this quenching is that Fe:ZnSe must be cryogenically cooled to achieve CW laser operation. However, room temperature operation has been demonstrated in gain switched operation with laser efficiencies of up to 34%.¹⁰

Many of the potential applications for mid-IR laser systems are in non-laboratory environments; hence, it is desirable for the laser to be vibrationally insensitive and to require minimal post-fabrication alignment. This criterion is not

often met by bulk laser systems, which include many free space optics. A monolithic waveguide design geometry allows the removal of the need for free-space optics in the laser system. ZnSe fiber is currently in development with propagation losses of <1 dB/cm at 1550 nm, but there is not yet any demonstration of transition metal doped ZnSe fibers lasing.¹¹ Thus, a solution is needed to leverage the advantages of waveguide geometry in the available bulk Fe:ZnSe polycrystalline laser samples. Macdonald *et al.*¹² were the first to demonstrate that ultra-fast laser inscription (ULI) could be used for fabrication of waveguides and waveguide lasers in Cr:ZnSe. ULI operates on the nonlinear absorption of a femtosecond pulse focused below the surface of a transparent dielectric. The high irradiances at the focus allow nonlinear processes such as multi-photon, tunnelling, and avalanche ionization to transfer energy to the material lattice.¹³ This energy transfer can result in a change of the refractive index at the focus of the laser beam. This index-modification can then be exploited to fabricate a waveguide. Later work by Macdonald *et al.* utilized the depressed cladding structures, first demonstrated by Okhrimchuk *et al.* in Nd:YAG,¹⁴ to demonstrate a Cr:ZnSe waveguide laser with a slope efficiency of 45%.¹⁵ This method makes use of a localized reduction in refractive index, and thus, the femtosecond laser is used to inscribe the cladding region of the waveguide. The advantage of this depressed cladding designs over that of positive index schemes, such as single line and multiscan modification,¹⁶ is the ability to arbitrarily change the diameter of the waveguide without developing any micro-cracking along the propagation of the waveguide. Micro-cracking has been observed with double clad multiscan waveguides in Cr:ZnSe.¹² The depressed cladding Cr:ZnSe waveguide laser has been demonstrated with a continuously tunable laser operation from 2077 to 2777 nm (Ref. 17) and power levels of 1.7 W.¹⁸ To the best of the authors' knowledge, there have not been any previous reports of waveguide fabrication in Fe:ZnSe by any method.

In this letter, we demonstrate a waveguide laser operation in Fe:ZnSe with a maximum power output of 76 mW. The advantages of longer interaction length between the

^{a)} Author to whom correspondence should be addressed. Electronic mail: a.k.kar@hw.ac.uk

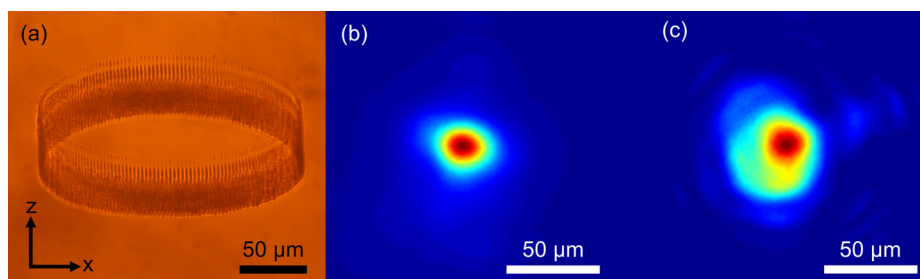


FIG. 1. (a) Optical micrograph of end facet of 200 μm wide waveguide. (b) Waveguide laser mode image at 4122 nm imaged at end facet when lasing from Fresnel reflection at output facet. (c) Bulk laser output mode at centered at 4135 nm lasing from Fresnel reflection at output facet.

pump and signal and tighter confinement resulted in a 44% reduction in laser threshold power. The laser emitted at a wavelength of 4122 nm with a FWHM linewidth of 6 nm. This is the longest output wavelength of any waveguide laser fabricated by ULI. The spectral width of a comparable bulk lasers system is found to be between 60 and 80 nm.¹⁹ The cause of this line narrowing in the depressed cladding waveguide is not yet fully understood, but it shows an unexpected advantage of this geometry.

A diffusion-doped polycrystalline Fe:ZnSe sample with dimensions 1.82 mm \times 4.76 mm \times 6.94 mm and a Fe²⁺ ion concentration of $8.88 \times 10^{18} \text{ cm}^{-3}$ was used to as a gain medium for the waveguide laser. The Fe:ZnSe sample used in this work was purchased from IPG Photonics. The waveguide structures created for this investigation were annular depressed cladding waveguides similar to that previously demonstrated in Cr:ZnSe, Cr:ZnS, and Tm:ZBLAN.^{15,20,21} The inscription laser used for this work was a Satsuma femtosecond laser by Amplitude Systems. Key material modification parameters such as pulse energy, pulse width, and the number of translations per element were investigated over a range of 1–2.1 μJ , 750–1000 fs, 100–200, and 1–9, respectively. For permanent negative refractive index change, pulse energies of 1.8 μJ were used with a temporal pulse width of 750 fs at a repetition rate of 100 kHz. The inscription beam was focused below the surface of the sample using a slightly over-filled 0.6 NA aspheric lens. The waveguides were inscribed along the longest dimension of the sample (6.94 mm). A range of waveguide horizontal diameters were investigated from 100 μm to 200 μm . The waveguides were inscribed with a sample translation speed of 9 mm/s in the y axis as shown in Figure 1. A microscope image of the end facet of a waveguide is shown in Figure 1(a). The NA of the Fe:ZnSe waveguides were measured directly from the output cone of light; direct measurement of the output mode produced an NA of 0.2. Clearly, the waveguide is smaller in the z-direction than the x-direction. Such asymmetric designs may be very useful to tailor the waveguide cross-section to match the asymmetry of diode pump sources.

For laser operation, the sample was placed inside an evacuated dewar as shown in Figure 2, with anti-reflective

(AR) coated CaF₂ windows. The sample was cooled to 77 K using liquid nitrogen. The sample chamber was put under vacuum to prevent condensation. A Sheamann MIR-PAC diode-pumped Er:YAG laser was used as the optical pump source for the laser, which was capable of 1.1 W CW at an emission wavelength of 2.94 μm . The pump laser beam was collimated using a 100 mm AR coated CaF₂ lens. A flat dichroic mirror was used as the rear laser mirror, which was AR coated for the pump and highly reflective ($R > 99.9\%$) at the lasing wavelength. A 35 mm focal length intra-cavity AR coated CaF₂ lens was used to focus the pump light onto the end facet of the waveguide. The output of the laser was collimated using an intra-cavity AR coated CaF₂ lens with focal length of 45 mm. An output coupling mirror was placed after the collimating lens.

Laser operation was obtained in many of the inscribed waveguides, the optimum of which had a core size of 151 μm and 40 μm in the x- and z-axes, respectively, as shown in Figure 1(a) with 200 inscription line elements and only one inscription translation per element. A range of output coupling was investigated using 80% and 90% reflective output couplers. The laser was also found to operate with feedback from the Fresnel reflection of the end facet ($R = 17.5\%$). For comparison, the sample was translated to a non-modified region in order to get the laser to operate in the bulk. For bulk laser operation, the intra-cavity input and output lens were translated towards the sample to have their focuses at the center of the sample. The performance of the waveguide and bulk laser is shown in Figure 3(a). Note that the values recorded for pump power have been reduced by the 17.5% Fresnel reflection at the input facet.

The optimum waveguide demonstrated an output power of 76 mW with a slope efficiency of 11.0% using an output coupler with $R = 80\%$. The threshold of laser action was found to be 210 mW. The lowest threshold of the waveguide laser was measured to be 153 mW with an output coupler with $R = 90\%$. There was no observed rollover at the highest pump power of 908 mW and thus, we can infer that that laser performance was pump limited and further power scaling is possible. In addition, for optimal laser performance, the Fe:ZnSe sample should be AR coated.

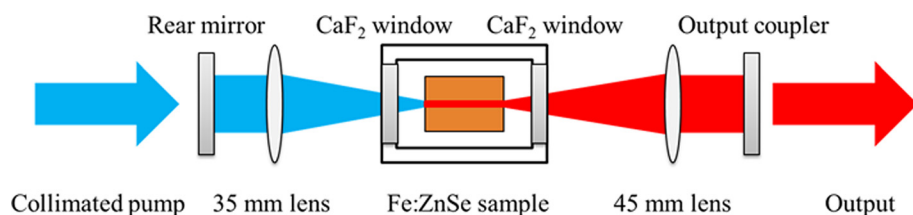


FIG. 2. Laser cavity configuration of Fe:ZnSe waveguide laser.

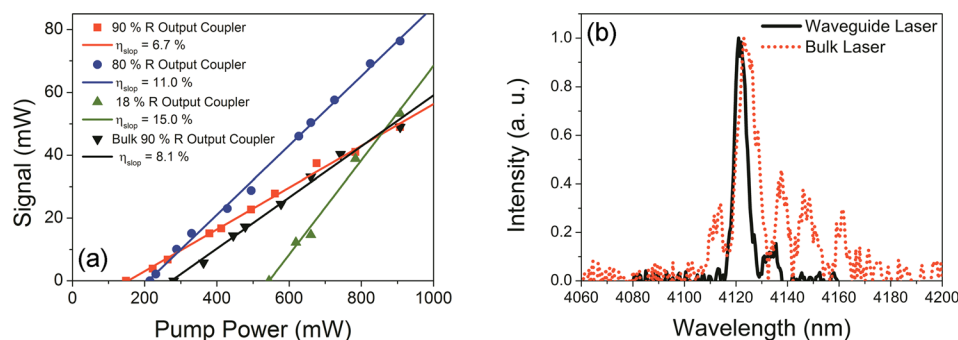


FIG. 3. Fe:ZnSe waveguide and bulk laser characterization. (a) Laser performance of waveguide and bulk Fe:ZnSe laser with different amounts of output coupling. (b) Spectrograph of Fe:ZnSe waveguide and bulk laser under 908 mW of pump power with a 80%R output coupler.

The laser output mode of the waveguide and bulk laser was imaged using a mid-IR camera (FLIR 7200) shown in Figure 1. The waveguide laser mode is near Gaussian with a FWHM of $63\ \mu\text{m}$ and $53\ \mu\text{m}$ in the x - and z -axes, respectively, in the plane of the output facet. The bulk laser mode is larger with a FWHM of $77\ \mu\text{m}$ and $90\ \mu\text{m}$ in the x - and z -axes, respectively, in the plane of the output facet. From Figure 1, we can conclude that transverse mode quality of the waveguide is superior to that of the bulk mode. The lower threshold of the waveguide laser is attributed to the smaller average mode size in the gain media and hence higher irradiance.

The spectra of the lasers were investigated using a monochromator (Gilden Photonics) with a spectral resolution of 0.4 nm. The spectra of the bulk and waveguide laser lasing with 906 mW of pump power are shown in Figure 3(b). The bulk emission consisted of multiple peaks spanning 50 nm, the largest centered at 4135 nm. This result is in good agreement with the work previously carried out in a bulk Fe:ZnSe laser by Evans *et al.*¹⁹ The waveguide laser was found to emit at a central wavelength of 4122 nm with a FWHM of 6 nm. It has been found experimentally that the spectral linewidth of the Cr and Fe doped depressed cladding waveguide lasers are considerably narrower than their typically bulk counterparts.^{15,22} Future work includes investigation of this interesting and very useful phenomenon, which is beyond the scope of this letter. Regardless, this is an additional benefit of the ULI waveguides, which will be useful for future sensing applications.

Direct comparison of the transmitted pump light under guiding and non-guiding conditions allowed an estimate of the waveguide losses due to increased scattering by the inscribed structures. With the pump laser operating at 450 mW and the Fe:ZnSe crystal cooled to 77 K, the pump light was launched into the inscribed waveguide. The power exiting the sample compartment was measured to be 0.865 mW. The sample compartment was translated, so that the beam propagated along a section of bulk Fe:ZnSe. In this configuration, the power exiting the sample compartment was measured to be 1.00 mW. The loss due to all effects, most notably, Fresnel effects and absorption of the pump radiation by the Fe^{2+} ions are the same in both configurations, so the difference in transmitted power is attributable to waveguide effects exclusively. Thus, the waveguide losses were calculated to be 0.91 dB/cm.

Additionally, the method of Findlay and Clay was used to find a value of the waveguide loss at the signal wavelength.²³ The modified Findlay–Clay equation was fitted to

the threshold and output coupler reflectivity data for the waveguide laser. Accounting for Fresnel reflectivity losses of 17.5% and 1.3% transmission losses of the CaF_2 windows, the propagation loss is calculated to be 0.16 dB/cm.

The scattering loss of the waveguide was also measured using the technique demonstrated by Okamura *et al.*²⁴ The output of a free-running Fe:ZnSe laser operating at approximately 4050 nm was launched into the waveguide, and the scattering from the side of the guide was imaged using a FLIR mid-IR camera. Image analysis of the scattered light enables a non-destructive technique for estimating losses from a waveguide structure. This image analysis technique eliminates the need to carefully factor out entrance and exit coupling losses required for input/output measurements. We also note from Ref. 7 that the absorption coefficient of Fe:ZnSe at 4050 nm at 77 K is negligible, so all the light image by the camera is from scattering processes. Using this method, the propagation loss in the waveguide at the signal wavelength is measured to be 0.46 dB/cm. The fidelity of this technique deteriorates when the signal to noise ratio is small, which is the case when the scattering losses are low. Consequently, the propagation losses calculated here should be interpreted as an upper-bound of the waveguide losses.

In summary, the value of the total waveguide loss was calculated using three methods. Direct measurement of the total loss at the pump wavelength gave a value of 0.9 dB/cm. Extrapolation of the value *in situ* with the laser running using the Findlay–Clay method gave a value of 0.16 dB/cm. The method of imaging scattered light at approximately the laser wavelength with an IR camera gave a value of 0.46 dB/cm. So, we see that each method indicates the total losses are <1 dB/cm, which is negligible compared with the small signal gain coefficient for our laser material, which is typically >20 dB/cm. Propagation losses of <1 dB/cm demonstrated in this paper are comparable to previous demonstrations of ULI passive waveguide devices at $4\ \mu\text{m}$.^{25,26}

In this letter, we have demonstrated a Fe:ZnSe waveguide laser. The waveguide structure was an annular depressed cladding structure fabricated by ULI. The inscribed waveguides were found to have a low propagation loss of <1 dB/cm at the lasing wavelength of 4122 nm. The laser emitted at a maximum output power of 76 mW, which was limited by the available pump power of 906 mW. The tighter confinement of the pump and laser signal beams by the waveguide resulted in a low laser threshold of 154 mW, which is a 44% reduction compared to an otherwise identical bulk system with a laser threshold of 274 mW. A narrow

spectral linewidth of 6 nm was demonstrated by the waveguide laser. To the best of the authors' knowledge, this is the narrowest linewidth demonstrated in any free-running Fe:ZnSe laser. Demonstration of an Fe:ZnSe laser in a guided-wave configuration will enable the creation of compact, all solid-state laser systems for commercial and laboratory use.

The authors acknowledge and thank support from AFRL Sensors Directorate, EOARD (Grant No. FA8655-1-3026) and EPSRC (Grant No. EP/G030227/1). A. Lancaster acknowledges support from EPSRC studentship EP/K502844/1.

- ¹L. D. DeLoach, R. H. Page, G. D. Wilke, S. A. Payne, and W. F. Krupke, *IEEE J. Quantum Electron.* **32**, 885–895 (1996).
- ²I. T. Sorokina, V. V. Dvoryn, N. Tolstik, and E. Sorokin, *IEEE J. Sel. Top. Quantum Electron.* **20**, 1–12 (2014).
- ³B. Meng and O. J. Wang, *J. Opt.* **17**, 023001 (2015).
- ⁴S. B. Mirov, V. V. Fedorov, D. Martyshkin, I. S. Moskalev, M. Mirov, and S. Vasilyev, *IEEE J. Quantum Electron.* **21**, 292–310 (2015).
- ⁵E. Sorokin, I. T. Sorokina, M. S. Mirov, V. V. Fedorov, I. S. Moskalev, and S. B. Mirov, in *Proceedings of Advanced Solid-State Photonics, San Diego, USA* (Optical Society of America, 2010), Paper No. AMC2.
- ⁶V. V. Fedorov, S. B. Mirov, A. Gallian, D. V. Badikov, M. P. Frolov, Y. V. Korostelin, V. I. Kozlovsky, A. I. Landman, Y. P. Podmar'kov, V. A. Akimov, and A. A. Voronov, *IEEE J. Quantum Electron.* **42**, 907–917 (2006).
- ⁷J. J. Adams, C. Bibeau, R. H. Page, D. M. Krol, L. H. Furu, and S. A. Payne, *Opt. Lett.* **24**, 1720–1722 (1999).
- ⁸D. V. Martyshkin, V. V. Fedorov, M. Mirov, I. S. Moskalev, S. Vasilyev, and S. B. Mirov, "High average power (35 W) pulsed Fe:ZnSe laser tunable over 3.8–4.2 μm ," in *Proceedings of CLEO: 2015, San Jose, California, USA* (Optical Society of America, 2015), Paper No. SF1F.
- ⁹V. Fedorov, D. Martyshkin, M. Mirov, I. S. Moskalev, S. Vasilyev, J. Peppers, S. B. Mirov, and V. P. Gapontsev, "Fe-doped II-VI mid-infrared

- laser materials for the 3 to 8 μm region," in *Proceedings of CLEO, San Jose, California, USA* (Optical Society of America, 2013), Paper No. JM4K.2.
- ¹⁰K. N. Firsov, E. M. Gavrishchuk, S. Y. Kazantsev, I. G. Kononov, and S. A. Rodin, *Laser Phys. Lett.* **11**, 085001 (2014).
- ¹¹J. R. Sparks, R. He, N. Healy, M. Krishnamurthi, A. C. Peacock, P. J. A. Sazio, V. Gopalan, and J. V. Badding, *Adv. Mater.* **23**, 1647–1651 (2011).
- ¹²J. R. Macdonald, S. J. Beecher, P. A. Berry, K. L. Schepler, and A. K. Kar, *Appl. Phys. Lett.* **102**, 161110–161113 (2013).
- ¹³R. R. Gattass and E. Mazur, *Nat. Photonics* **2**, 219–225 (2008).
- ¹⁴A. G. Okhrimchuk, A. V. Shestakov, I. Khrushchev, and J. Mitchell, *Opt. Lett.* **30**, 2248–2250 (2005).
- ¹⁵J. R. Macdonald, S. J. Beecher, P. A. Berry, G. Brown, K. L. Schepler, and A. K. Kar, *Opt. Lett.* **38**, 2194–2196 (2013).
- ¹⁶H. T. Bookey, R. R. Thomson, N. D. Psaila, A. K. Kar, N. Chiodo, R. Osellame, and G. Cerullo, *IEEE Photonics Technol. Lett.* **19**, 892–894 (2007).
- ¹⁷J. R. MacDonald, S. J. Beecher, A. Lancaster, P. A. Berry, K. L. Schepler, and A. K. Kar, *IEEE J. Sel. Top. Quantum Electron.* **21**, 1601405 (2014).
- ¹⁸P. A. Berry, J. R. Macdonald, S. J. Beecher, S. A. McDaniel, K. L. Schepler, and A. K. Kar, *Opt. Mater. Express* **3**, 1250–1258 (2013).
- ¹⁹J. W. Evans, P. A. Berry, and K. L. Schepler, *Opt. Lett.* **37**, 5021–5023 (2012).
- ²⁰J. R. Macdonald, S. J. Beecher, A. Lancaster, P. A. Berry, K. L. Schepler, S. B. Mirov, and A. K. Kar, *Opt. Express* **22**, 7052–7057 (2014).
- ²¹D. G. Lancaster, S. Gross, H. Ebendorff-Heidepriem, K. Kuan, T. M. Monro, M. Ams, A. Fuerbach, and M. J. Withford, *Opt. Lett.* **36**, 1587–1589 (2011).
- ²²P. A. Berry and K. L. Schepler, *Opt. Express* **18**, 15062–15072 (2010).
- ²³D. Findlay and R. A. Clay, *Phys. Lett.* **20**, 277 (1966).
- ²⁴Y. Okamura, S. Yoshinaka, and S. Yamamoto, *Appl. Opt.* **22**, 3892–3894 (1983).
- ²⁵Q. An, Y. Ren, Y. Jia, J. R. V. D. Aldana, and F. Chen, *Opt. Mater. Express* **3**(4), 466–471 (2013).
- ²⁶S. Gross, N. Jovanovic, A. Sharp, J. Lawrence, and M. J. Withford, *Opt. Express* **23**, 7946–7956 (2015).